The design of advanced performance high strength low-carbon martensitic armour steels: Microstructural considerations

Kasonde Maweja[a] and Waldo Stumpf[a]

[a] Department of Materials Science and Metallurgical Engineering, **University of Pretoria**, 0002 Pretoria, South Africa

.

Abstract

Neither a higher hardness nor higher mechanical properties (yield strength, ultimate tensile strength, impact energy, and %elongation) appear to be exclusive or even reliable criteria for predicting the ballistic performance of martensitic armour steels, as shown in our previous work [K. Maweja, W.E. Stumpf, Mater. Sci. Eng. A (February), submitted for publication]. An alternative design methodology for tempered martensitic armour steels is, therefore, proposed which is based on the effect of retained austenite on the ratio of the yield to ultimate tensile strength (YS/UTS), the microstructure of the tempered martensite and its martensite start temperature M_s. This approach was developed using 6 mm thick armour plates and later was successfully applied to the design of eight experimental armour steels with plate thicknesses ranging from 4.7 to 5.2 mm and tested by the standard R4 (5.56 mm rounds) ballistic test.

Article Outline

1. Introduction

Over the last few decades military and security specifications have been developed for armour steel plates based on their predicted behaviour when impacted by high velocity rounds. Hitherto the hardness and the tensile and impact properties (in particular, the yield strength, the ultimate tensile strength, the elongation at room temperature and the transverse Charpy-V impact energy at −40 °C) were the main design parameters for most armour steel plates [1], [2] and [3]. Current specifications for military and security applications recommend a minimum Brinell hardness range of 540–600 BHN [1] or 55–60 Rockwell C [2], and a minimum yield and ultimate tensile strength of 1500 and 1700 MPa, respectively, while a minimum transverse Charpy-V impact energy of 13 J at −40 °C and a minimum elongation of 6% (50 mm gauge length) is required in South Africa [1]. These requirements have been successfully achieved over many years by a suitable combination of chemical composition and heat treatment parameters of armour steels for plates generally thicker than 8.5 mm up to 30 mm.

Recent work by Maweja and Stumpf [4] and [5] and other authors [6], [7] and [8], however, has shown that the hardness of the target steel, contrary to the above specifications, was not the all-important factor that determines the resistance to ballistic perforation. The yield and the ultimate tensile strength, rather than the hardness, are considered to be more important in approximating the true dynamic fracture and spalling strength of the armour steel. Accurate measurements of dynamic stresses upon ballistic impact have detected stresses as high as 28 GPa (which was the measurement limit in that case) before fracture of the bainitic steel plates occurred where the tensile strength at low strain rates was only about 2 GPa [9].

Srivathsa and Ramakrishnan [6] and [7] have proposed a model for the calculation of the ballistic impact energy per unit area-density and have defined a ballistic performance index (BPI) for predicting the performance of armour plates. The variables in the BPI are the steel density, elastic modulus, the yield and tensile strength, Poisson's ratio, the reduction in area or the fractional elongation during impact and V_0, the striking velocity of the fired round. The BPI contains terms that represent the elastic and the plastic components of the strain energy, and a last term corresponds to the kinetic energy of the system target-round after impact. All the parameters considered in the BPI model are measured under low strain rates at room temperature.

Dikshit et al. [10] ballistically studied thick steel plates over the velocity range 300–800 m/s and concluded that the effect of hardness of a plate on its ballistic performance depended on whether the stress state was predominantly plane strain or plane stress. At hypervelocity impact in the range of 1.5–4 km/s, Sorensen et al. [11], observed that, despite its lower hardness, nitrogen alloyed austenitic steels exhibited the same ballistic performance than high strength armour steel.

The effect of the hardness on the ballistic performance of armour steels is, therefore, not uniquely defined. It depends on the strain rate (function of the striking velocity) and the thickness of the plate. It appears that in thicker plates and under low strain rates that the

ballistic affected region is more localised than in thinner plates. Therefore, the ability to resist ballistic perforation depends on the hardness in the first case, whereas the ability to deform plastically in a large volume around the impact region become the determinant in the case of thinner plate's performance under high strain rates.

In previous work [4], the thermal effect and the subsequent phase transformations and transitions that occur when high velocity rounds impact on martensitic steel armour plates and which are not accounted for in the BPI model, were presented. Transmission electron microscopy of the ballistic impact regions in eight armour steels suggested that the thermal effect that accompanies the impact and the subsequent phase transformations, might absorb a significant part of the kinetic energy of fired rounds and consequently improve the resistance to ballistic perforation. It would then become necessary to account for these phenomena in the models for an improved prediction of the ballistic performance, allowing the design of higher performance martensitic armour steels.
In this paper, the aim was to develop an approach for the design of advanced performance martensitic armour steels from microstructural considerations. This approach has the benefit of overcoming the lack of correlation between high strength and high ballistic performance as recently observed by us [5] and many other researchers [12], [13], [14], [15], [16] and [17]. The discrepancies between mechanical properties and ballistic performance in the case of martensitic armour steels were analysed and possible explanations given in more detail somewhere else [5].

A phenomenon of great importance during ballistic impact is the formation of the shear bands. In their study on the effect of strain rate upon plastic flow of steel, Zener and Hollomon [20] stipulated that adiabatic heating may occur whereby the heat generated during the deformation is restrained in a particular region causing a local rise in temperature. When the local condition is such that the effect of thermal softening due to the adiabatic heating is greater than the strain-hardening effect of the deformation, a condition of thermo-mechanical instability resulting in a highly localised plastic shear strain occurs. The formation of the adiabatic shear bands (ASBs) and their role into the failure mechanism of high velocity impacted targets, ballistic impact, explosive fragmentation, cryogenic behaviour of materials and high speed machining have been the objects of many current research works.

Odeshi et al. [21] and [22] used the split Hopkinson pressure bar (SHPB) and investigated into the role of the ASBs in the failure mechanism of a high strength low alloy steel at high strain rate of about 1.9×10^3 s^{-1}. They suggest that the deterioration of material properties occurred as a result of adiabatic shearing during high strain-rate deformation. Micropores that form during thermal softening of the steel in the ASB during impact initiate the process that eventually leads to fragmentation of the samples. The micropores coalesce to form voids, which serve as nucleating point for cracks. Most material failures at high strain rate are usually preceded by adiabatic shear band formation. Perforations of steel shells by ballistic impact as well as fragmentation of steel casement after explosion are usually explained in terms of shear strain localization [23] and [24].

Follansbee and Gray [25] found deformation twins Ti-6Al-4V only at very high strain rate (5000 s^{-1}) and low temperatures. However, in the case of low strain rates and high temperatures, dislocation motion is the dominating component in the deformation mechanism of the alloys through planar slips with negligible amounts of twin deformation.

2. Materials and experiments

2.1. Chemical composition and manufacturing

Five experimental armour steels, namely steels G1A through to G3 were subjected to standard ballistic testing and their performance compared to those of three currently produced and used armour steels, here named A66, M38 and RL5. Their chemical compositions, casting details, hot rolling processes, heat treatments and the specifications of the ballistic testing applied to these steels are described in Ref. [5].

3. Results of the ballistic testing

3.1. The ballistic parameter (BP)

The results on the ballistic performance of these eight martensitic steels are presented again in Table 1. It was observed in Part 1, of this work, that the prediction of the ballistic performance of martensitic armour steels based on their tensile properties as measured at "lower" strain rates at room temperature, or on the hardness and Charpy impact energy at −40 °C was not accurately defined [5].

Table 1.
Results of the ballistic testing

Steel designation	Firing distance (m)	Ballistic performance
G1A	30	Passed
G1A	10	Passed
G1B	30	Passed
G2A*	30	3 out of 5 failed
G2B**	30	Failed
G3**	30	Failed
A66	30	Passed
M38	30	Passed
RL5**	30	Failed

Note: In the rest of this paper (as also in Part 1) the steels will be designated with (i) no asterisk = passed, (ii) one asterisk = partially failed and (iii) two asterisks = failed the ballistic test.

An alternative ballistic parameter was proposed to account for the microstructural and the plate thickness effects in predicting the ballistic performance, based on the experimental results on a further 13 martensitic armour steels [4]. The BP was defined as follows:

$$BP = \frac{RA(\%)}{\exp(\delta)} \quad (1)$$

where RA is the volume fraction of the retained austenite in the martensitic microstructure and δ is the thickness of the plate in millimetres. The choice of this expression for the BP parameter is based on the proportional lowering of the yield to ultimate tensile strength ratio (YS/UTS) by the presence of retained austenite in the microstructure and on the increase of the effective penetrating mass when the thickness of the plate increases because of the direct transmission of the linear momentum to the cylinder of material ahead of the fired round within the plate.

The ballistic parameters of the experimental plates of interest are compared in Table 2.

Table 2.
Ballistic parameter, YS/UTS and ballistic performance

Name of the steel	**RA (vol%)**	δ	**BP**	**YS/UTS**
G1A	6.0 ± 0.5	6.0 ± 0.2	0.015	0.50
G1B	4.0 ± 0.5	6.0 ± 0.2	0.010	0.58
G2A*	0.6 ± 0.5	6.0 ± 0.2	0.0015	0.68
G2B**	0.6 ± 0.5	6.0 ± 0.2	0.0015	0.75

The 6 mm thick plate of steel G2A* (Group 2) withstood only two of the five rounds fired and, therefore, constituted the demarcating case between those that passed (Group 1) and those that completely failed the ballistic test (Group 3). The ballistic parameter limit value of 0.010, corresponding to the plate of steel G1B, was then used for subsequent predictions of the ballistic performance of armour plates with thicknesses smaller than 6 mm and was successfully applied to eight further experimental advanced performance steel armour plates with thicknesses ranging from 4.7 to 5.2 mm [4], whilst keeping the ballistic test conditions unaltered.

The BP can be considered as an attempt to find a *direct relationship* between the microstructure and the ballistic performance instead of an *indirect relationship* via the mechanical properties. The BP was used for the design of eight further experimental

martensitic armour steels with thicknesses in the range 4.7–5.2 mm [4]. It was observed that plates with BP higher than a value of 0.010 passed the ballistic test, those with a BP near to 0.006 also passed the ballistic test, but dynamic cracks were found to propagate while those plates with a BP ≈ 0.003 failed the ballistic test. It was also observed that the subsequent plastically deformed area around the impact regions increased as the BP increased within the limits of the experiments.

It may also be observed that steels G1A and G1B had values of the yield to ultimate tensile strength ratio (YS/UTS) close to 0.6. These lower values of this ratio indicate the steel's ability to resist localised yielding; in other words, it indicates the ability of the material to dissipate the absorbed kinetic energy through a larger plastic strain around the impact area. This property increases the volume of the material interacting with the fired round, offering better resistance to perforation. The elongation during uniaxial tensile testing indicates the tendency for localised yielding of the steel when impacted. It should be kept lower than 7% [5]. This observation seems contrary to the current specification that recommends an elongation higher than 6% for martensitic armour steel plates thicker than 12 mm [1].

3.2. Microstructure

Thin foil transmission electron micrographs of the armour steels G1A, G1B, G2A* and G2B** before ballistic testing are compared in Fig. 1(a) through to (c) after a prior tempering at 180 °C for one hour. This tempering temperature was found to be the most optimum for the above three steels (Groups 1 and 2) for achieving a high ductility at room temperature [5]. Fine elongated strings of carbides were found in twinned martensite plates of steels G1A and G1B that were aligned parallel to the martensite plate interfaces as illustrated in Fig. 1(a) of these two steels that later passed the ballistic test. On the other hand, coarse carbides had precipitated within the martensite laths and on the lath interfaces of steels G2A* and G2B** and these gave poor ballistic performances.

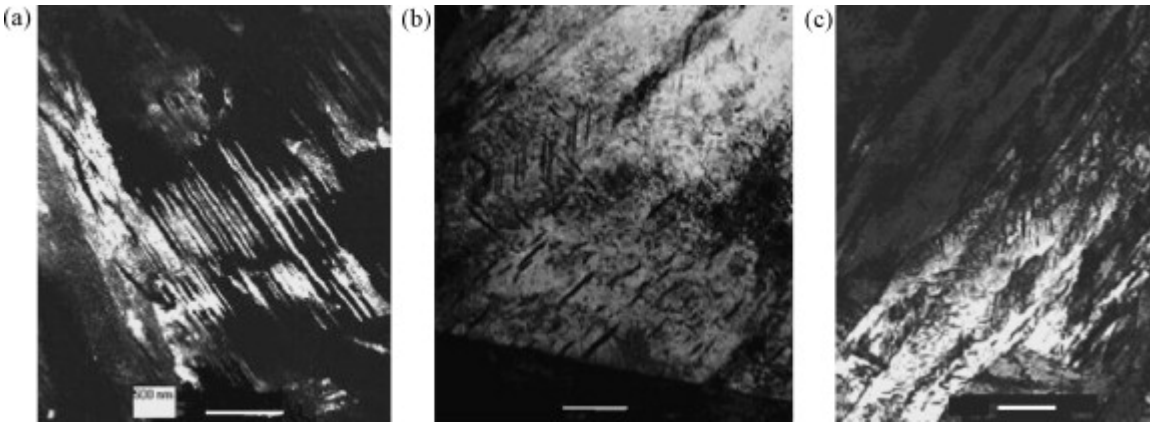

Fig. 1. Thin foil transmission electron microscopy of steels (a) G1A, (b) steel G2A* and (iii) steel G2B** after tempering at 180 °C and before ballistic testing. Scale bar length = 500 nm.

It is inferred from Fig. 1 that a high ballistic performance requires a microstructure consisting of twinned martensite with some retained austenite without coarse carbides. The precipitation of heavy cementite should be avoided by controlling the chemical composition, i.e. through the silicon content of the steel and the tempering temperature. Steels G1A and G1B that gave successful ballistic performances after quenching and tempering at 180 °C for one hour, were also tempered at higher temperatures of up to 400 °C to find the upper limit of tempering before the detrimental coarse cementite starts to make its appearance. After tempering at 300 °C for 1 h the TEM thin foil micrographs in Fig. 2 show large strings of coarse cementite that formed along the plate interfaces of the steel G1A with 0.21 wt% Si, while in steel G1B with 1.06 wt% Si, noticeably less of these coarse strings of carbides were formed. Hence it is likely that steel G1B will still have a satisfactory ballistic performance, even after tempering at a relatively higher temperature.

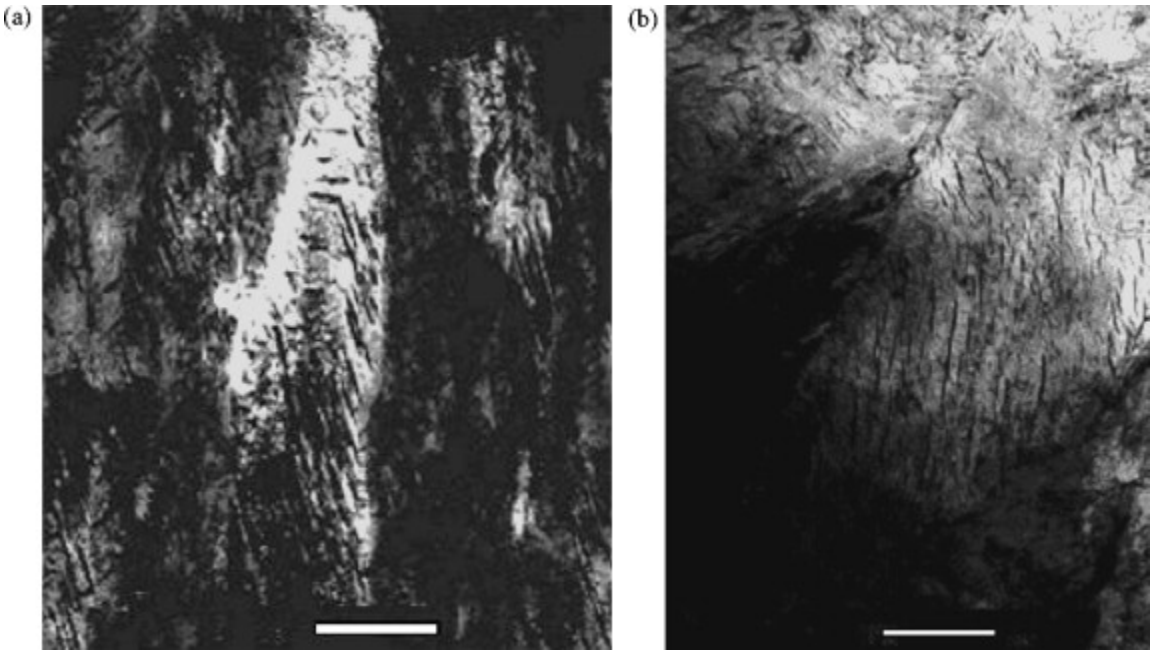

Fig. 2. Bright field thin foil transmission electron micrographs of steels G1A and G1B after tempering at 300 °C. (a) Steel G1A (0.21 wt% Si) and (b) steel G1B (1.06 wt% Si).

The retardation in the formation of coarse cementite during tempering of steel G1B can be attributed to its higher content of 1.06 wt% silicon, an element that is well known for its effect on delaying the formation of cementite from supersaturated metastable martensite [18]. Tempering at 400 °C is not acceptable even for armour steels containing more than 1 wt% silicon because of the significant softening of the material and the formation of coarse cementite, as shown in Fig. 3.

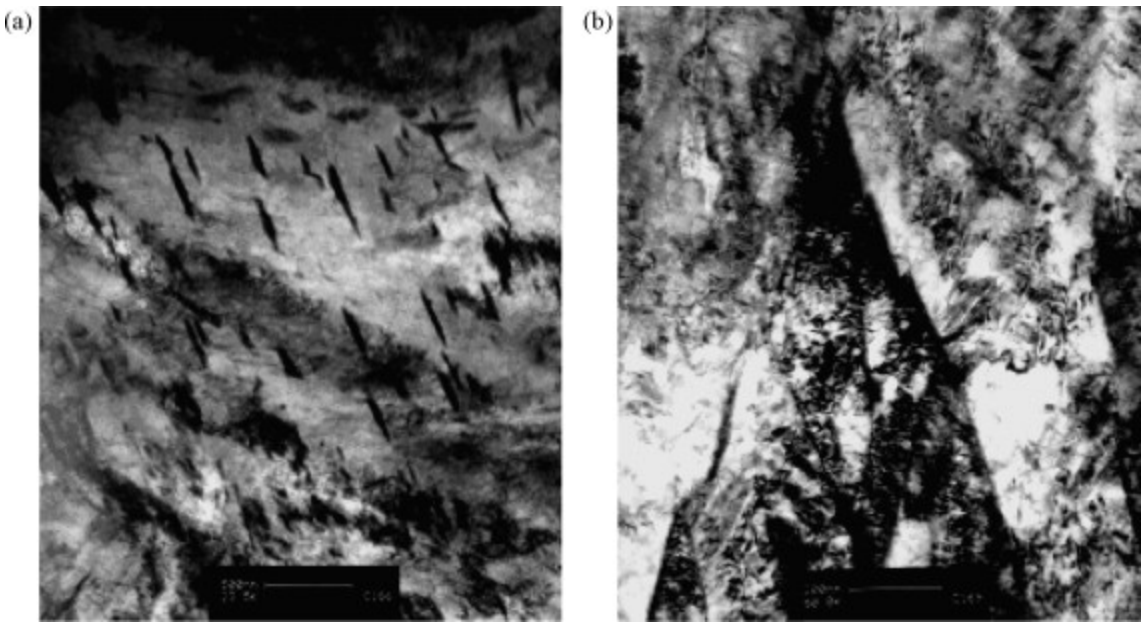

Fig. 3. (a) Bright field thin foil TEM of steel G1A (0.21 wt% Si) tempered at 400 °C showing large strings of cementite. (b) Bright field thin foil TEM of steel G1B (1.06 wt% Si) tempered at 400 °C showing coarse cementite.

With tempering at 400 °C, strings of cementite in the steel G1A (with lower %Si) are formed which coarsened along parallel directions contrary to the dispersed particles of cementite that precipitated in the steel G1B with its higher %Si.

3.3. The martensite start temperature of the steel

M_s temperatures of the martensitic armour steels were estimated, with an absolute error of ±15 °C, using the regression formula (3.1), which was based on 23 measured values using dilatometry for armour steels within the range of chemical compositions (in wt%) of interest here [19].

$$M_s\ (°C)=548–590C–35Mn–18Ni–14Cr–9.5Mo–12Si \tag{3.1}$$

The effect of the austenitisation temperature on the martensite start temperature was also analysed for these armour steels in the range between 800 and 950 °C, austenitised for 10 min in each case. The martensite start temperatures of these armour steels decrease slightly, typically by about 6–10 °C when the austenitisation temperature is increased from 800 to 950 °C [19]. The increase in the austenitisation temperature has many consequences, i.e. greater dissolution of carbides, more solid solution hardening of the parent austenite as well as austenite grain growth and all of these can modify the martensitic transformation process. For instance, greater dissolution of the carbides changes the chemical composition of the matrix and, hence, the chemical driving force for the transformation of the austenite into martensite. It also increases the solid solution hardening of the parent austenite, which affects the movement of the dislocated transformation front through the harder austenite.

4. An improved design scheme for advanced performance armour steels

An improved design scheme for high ballistic performance martensitic armour steels should consider the following.

4.1. The chemical composition of the steel and its tempering treatment

a. Carbon is the main alloying element that determines the hardness of the martensite. A hardness higher than 500 VHN may be obtained when the carbon content of the armour steel is above 0.37 wt% C.
b. The silicon content of the steel has a strong effect on the stability of the martensite upon tempering, as it delays the softening of the martensite during tempering at higher temperatures. It also appears to increase the resistance to dynamic coarsening of the cementite upon ballistic impact [4].

Softening of these martensitic steels upon tempering gave the following threshold temperatures where the hardness started to drop measurably.

Silicon increases the stability of the martensite by reducing the chemical activity of carbon [18] and, therefore, becomes effective in delaying the decomposition of the martensite in steels in the range between 0.5 and 1.0 wt% C. However, from Table 3 it appears that the stability of the martensite upon tempering does not correlate uniquely with the M_s of the steel.

Table 3.
Silicon content and the temperature of softening of the martensite in five experimental armour steels

Steel	Si (wt%)	M_s (°C)	Tempering temperature of measurable softening (°C)
G1A	0.21	196	180
G3	0.40	309	200
G2B	0.43	271	200
G2A	0.8	255	250
G1B	1.06	212	300

c. The martensite start temperature of these armour steels may be approximated with acceptable accuracy using the experimentally determined regression formula (3.1).
d. Higher volume fractions of retained austenite in twinned plate martensite lead to lower values of the YS/UTS and to an improved ballistic performance.

4.2. The microstrural-based design procedure for low-carbon martensitic plates with thickness less than 8.5 mm

The microstrural-based design procedure for advanced performance tempered low-carbon martensitic armour steels (Group 1) and for high strength components (Group 2) will consist of the following five steps:

Step 1: *The chemical composition*

Select the chemical composition (in wt%) of the steel within the following range: 0.37–0.43 wt% C, 0.5–1.8 wt% Mn, 0.6–1.2 wt% Si, 0.8–1.5 wt% Cr, 0.5–0.6 wt% Mo, 1.8–4.0 wt% Ni with the final chemical composition chosen such that the martensite start temperature corresponds to the following classification and probable areas of application (Table 4).

Table 4.
Classification of martensitic armour steels

	M_s (°C)	**Thickness of armour plates (mm)**	**Application**
Group 1	<210	4.5–6	High ballistic performance
Group 2	210 <M_s < 260	8.5–20	High strength and medium ballistic performance
Group 3	>260	30	High toughness and poor ballistic performance

The M_s temperature of the steel may initially be approximated using formula (3.1), during the design process but later a measured value should be obtained by dilatometry analysis.

Step 2: *The heat treatment*

The austenitisation temperature and the tempering temperature will determine the final properties of the martensitic steels. The austenitisation conditions have an effect on the M_s temperature, hence on the thermodynamics and kinetics of the martensite transformation, and on the microstructure (Table 5).

Table 5.
Optimum heat treatment and microstructures

	High performance armour plates	**High strength components**
Category	Group 1	Groups 2
Austenitisation	870–950 °C for 20–60 min	800–860 °C for 20–60 min
Quenching medium	Water at room temperature	Water or oil

	High performance armour plates	**High strength components**
Tempering	150–200 °C for 20–30 min	250–300 °C for 20–30 min
Retained austenite	1–7% volume fraction	Not necessary
YS/UTS	<0.6	>0.75
Microstructure	Twinned plate martensite with nodular retained austenite	Butterfly and lath martensite without retained austenite
Detrimental particles	Coarse cementite	Elongated manganese sulphide, other inclusions and cementite when the tempering temperature increases
Strain rate	Very high	Low

Step 3: *Prediction of the ballistic performance*
Perform a phase analysis by XRD, determine the volume fraction of retained austenite and calculate the BP of the plate. The minimum required BP should be equal to 0.010.
Step 4: *Assessment of the performance and failure mode*
Perform a standard ballistic test to confirm the performance prediction on armour plate having BP values higher than 0.010.

Bassim [26] used a torsional split Hopkinson bar system to investigate the formation and evolution of ASBs at high strain rate in AISI 4340 steel. He suggested that ASB initiate at local defects and inhomogenities in the material. The specimen geometry and dimensions are also contributing factors in the development of ASBs.

Roessig and Mason [27] noticed that the failure mode in quasistatic and low velocity tests of 1018 steel was tensile and not shear dominated. At higher impact speed, however, the 1018 steel begin to show evidence of a transition to shear dominated failure. They also suggested that the high concentration of precipitates causes the strengthening of an aluminium matrix and prevents the large plastic deformation needed to generate enough heat for a thermal softening process to take over, thus, no adiabatic shear localization occurs.

The effect of strain rate on the role of inclusions, manganese sulphide, was illustrated using scanning electron microscopy [5]. It was also shown that intergranular cracks propagated forming a chevron pattern through the thickness of the untempered armour plate, with some grains being pulled out, before a catastrophic failure occurred. It is inferred from the TEM illustrating the changes in microstructure upon ballistic impact that the size of the thermally affected zone depends on the chemical composition of the armour steel. The size of the plastic zone depends on the initial microstructure [4] and

[5]. Therefore, the threshold of the adiabatic shear bands initialisation may be chemistry dependent. However, there sizes and shapes may be microstructure dependent.

Step 5: *Microstructure analysis*
Perform TEM and XRD analysis to confirm the dependence of the ballistic performance on the microstructure and phases present.

The proposed design scheme was successfully applied to the design of a further eight experimental martensitic armour steels with plate thicknesses ranging between 4.7 and 5.2 mm and BP values ranging between 0.006 and 0.055 and fully reported in Ref. [4]. The ballistic behaviour and the phenomenological explanations of their enhanced performance of those steels have been fully addressed in our previous work [4].

5. Conclusion

1. It is possible to predict the ballistic performance of martensitic armour steels by considering the microstructure, morphology and the phases inherited from the combination of chemical composition and heat treatment. The BP, which includes the volume fraction of the retained austenite in these steels and the M_s temperature, which determines its morphology, can be considered as criteria for the classification of martensitic armour steels in three application groups.

2. The microstructure-based design scheme has the advantage of addressing a direct relationship between the microstructure and ballistic performance instead of an uncertain and disproven indirect relationship through the mechanical properties.

3. For a given chemical composition, it is possible to design for a high ballistic performance or for high strength depending on the heat treatment parameters; a lower YS/UTS ratio indicates a higher resistance to localised yielding upon impact, hence an improved resistance to ballistic perforation for a given composition of the martensitic steel.

References

[1] Mittal Steel, personal communication, 2004.

[2] H. Kolsky In: R.C. Laible, Editor, *Ballistic Materials and Penetration Mechanics* (1982), pp. 160–190.

[3] F. Hallock In: J.A. Zukas, T. Nicholas and F.S. Hallock, Editors, *Impact Dynamics*, John Wiley and Sons (1982), pp. 215–230.

[4] K. Maweja and W.E. Stumpf, *Mater. Sci. Eng. A* **432** (2006), pp. 158–169.

[5] K. Maweja, W.E. Stumpf, doi:10.1016/j.msea.2007.08.048.

[6] B. Srivathsa and N. Ramakrishnan, *J. Mater. Process. Technol.* **96** (1999), pp. 81–91.

[7] B. Srivathsa and N. Ramakrishnan, *Comput. Simul. Modell. Eng.* **3** (1998), pp. 33–40.

[8] N. Ramakrishnan, Ballistic Test Procedures for Armour Materials Technical Report DMRL, Hyderabad, India, 1986.

[9] R.I. Hammond and W.G. Proud, *R. Soc.* **460** (2004), pp. 2959–2974.

[10] S.N. Dikshit, V.V. Kutumbarao and G. Sundararajan, *Int. J. Impact Eng.* **16** (2) (1995), pp. 293–320.

[11] B.R. Sorensen, K.D. Kimsey, G.F. Silsey, D.R. Scheffler, T.M. Scherrick and W.S. de Rosset, *Int. J. Impact Eng.* **11** (1) (1991), pp. 107–119.

[12] T. Borvik, M. Langseth, O.S. Hopperstad and K.A. Malo, *Int. J. Impact Eng.* **22** (1999), pp. 855–886.

[13] T. Borvik, O.S. Hopperstad, T. Berstad and M. Langseth, *Eur. J. Mech. A/Solids* **20** (2001), pp. 685–712.

[14] T. Borvik, O.S. Hopperstad, T. Berstad and M. Langseth, *Eur. J. Mech. A/Solids* **22** (2003), pp. 15–32.

[15] S. Dey, T. Borvik, O.S. Hopperstad, J.R. Leinum and M. Langseth, *Eng. Fract. Mech.* **70** (2003), pp. 2543–2558.

[16] I. Mescheryakov Yu, A.K. Divakov and N.I. Zhigacheva, *Int. J. Solids Struct.* **41** (2004), pp. 2349–2362.

[17] Z. Rosenberg and E. Dekel, *Int. J. Impact Eng.* **30** (2004), pp. 835–851.

[18] H.K.D.H. Bhadeshia, *Metal Sci.* **17** (1983), p. 151.

[19] M. Kasonde, MEng thesis, University of Pretoria, 2005.

[20] C. Zener and J.H. Hollomon, *J. Appl. Phys.* **15** (1944), pp. 22–32.

[21] A.G. Odeshi, M.N. Bassim, S. Al-Ameeri and Q. Li, *Mater. Process. Technol.* **169** (2005), pp. 150–155.

[22] A.G. Odeshi, M.N. Bassim and S. Al-Ameeri, *Mater. Sci. Eng. A* **419** (2006), pp. 69–75.

[23] S.E. Schoenfeld and T.W. Wright, *Int. J. Solids Struct.* **40** (2003), pp. 3021–3037.

[24] M.N. Raftenberg and C.D. Krause, *Int. J. Impact Eng.* **23** (1999), pp. 757–770.

[25] P.S. Follensbee, Part 1, Experimental investigation, *Int. J. Plasticity* **15** (1999), pp. 241–262.

[26] M.N. Bassim, *Mater. Process. Technol.* **119** (2001), pp. 234–236.

[27] K.M. Roessig and J.J. Mason, *Int. J. Plasticity* **15** (1999), pp. 241–262.

Corresponding author. Present address: Council for Scientific and Industrial Research (CSIR), CSIR/MSM/MMP, PoB 395, Pretoria 0001, South Africa. Tel.: +27 83 365 0952; fax: +27 12 362 5304.